Mechanistic Insights into the Synthesis of Higher Alcohols from Syngas on CuCo Alloys

Ang Cao,[†,‡,§] Julia Schumann,[‡,§] Tao Wang,[‡,§] Linan Zhang,[‡,§] Jianping Xiao,[‡,§] Pallavi Bothra,[‡,§] Yuan Liu,[†] Frank Abild-Pedersen,[*,‡,§] and Jens K. Nørskov[*,‡,§]

[†]School of Chemical Engineering and Technology, Tianjin University, Tianjin 300072, People's Republic of China

[‡]SUNCAT Center for Interface Science and Catalysis, SLAC National Accelerator Laboratory, Menlo Park, California 94025, United States

[§]SUNCAT Center for Interface Science and Catalysis, Department of Chemical Engineering, Stanford University, Stanford, California 94305, United States

ABSTRACT: Synthesis gas ($CO + H_2$) conversion is an important process in the transformation of coal, natural gas, or biomass into higher-value products. The explicit conversion into C_{2+} oxygenates on transition-metal-based catalysts suffers from a low selectivity, being a consequence of an imperative integration of C−O bond splitting and C−C coupling reactions. Recently, it has been demonstrated that a bimetallic CuCo catalyst has high higher alcohol selectivity under mild reaction conditions, but the details of the reaction mechanism on the surface are still elusive. In this work, we studied the formation of methane, methanol, and ethanol from syngas on a close-packed (111) and a stepped (211) CuCo surface combining density functional theory (DFT) and microkinetic modeling. We found the CuCo alloy to be a promising candidate catalyst, displaying the required coverage of CO and CH_x on the surface to facilitate C−C coupling. In addition, we found the selectivity to be very structure sensitive: the CuCo (211) surface is selective toward ethanol under certain reaction conditions, while the (111) surface is selective toward methanol. We identified the much lower C−O dissociation barrier and the higher rate of CH_x−CO coupling as the reason for the high activity and selectivity toward ethanol on the (211) surface.

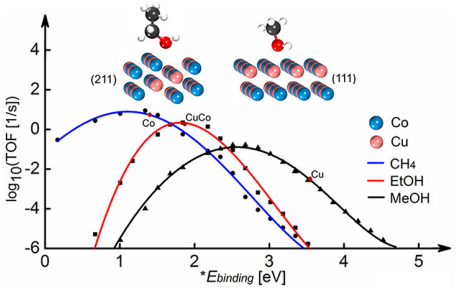

KEYWORDS: *synthesis gas conversion, higher alcohol synthesis, CuCo alloy, DFT, microkinetic modeling*

1. INTRODUCTION

Higher alcohol synthesis (HAS) via syngas produced from coal, natural gas, or renewable biomass has drawn considerable attention due to its potential as a transportation fuel, as a gasoline additive or as an intermediate for other chemicals.[1−3] The process is competing with a number of side reactions, Fischer−Tropsch (F-T) synthesis, methanation, methanol synthesis, and the water-gas shift reaction, which can lead to a very diverse distribution of products depending on the catalysts.[4] Therefore, it is of central importance to understand the underlying atomistic and electronic structure factors that determine the activity and selectivity in syngas conversion processes if one wants to design catalysts with a high selectivity toward higher alcohols.

It is widely accepted that methanol is produced by the hydrogenation of nondissociated CO, while methane and higher hydrocarbons are formed by the hydrogenation of the surface hydrocarbon species (CH_x), which is produced by a direct or hydrogen-assisted dissociation of CO.[5−7] The formation of higher alcohols requires the insertion of CO into CH_x to give an acyl intermediate that subsequently can form an alcohol molecule by hydrogenation.[8,9] An efficient HAS catalyst therefore needs elements of both the methanation and the methanol synthesis catalyst.

For one of the most promising CuCo-based catalysts, it has been shown that step sites on the Cu surface are responsible for the methanol formation,[10,11] whereas Co sites efficiently dissociate CO and therefore mainly produce CH_4 and other hydrocarbons.[12] Therefore, we suggest that the synergistic working of the copper and cobalt sites may be crucial in the selectivity toward higher alcohols.[13,14] In previous work[15,16] CuCo alloy surfaces were successfully prepared by calcining and reducing layered double hydroxide (LDHs) precursors, and a high activity and selectivity toward C_{2+} alcohols was found. Tien-Thao et al.[17,18] have also reported that the Co-Cu alloy, formed by the reduction of a $LaCo_{1-x}Cu_xO_3$ perovskite precursor, is a prerequisite for a higher alcohol synthesis catalyst. The synergetic effect of Cu and Co atoms is believed to form the active sites for HAS on the CuCo-based catalysts.

Research on improving the catalytic performance of the CuCo alloy catalysts has mainly focused on varying catalyst

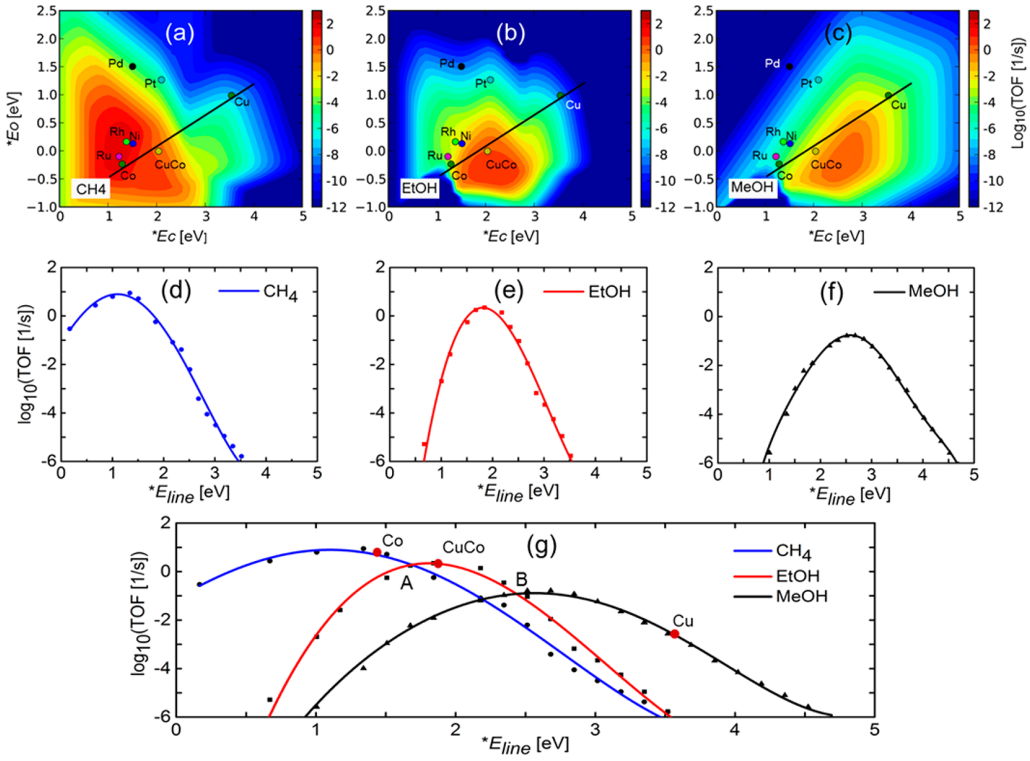

Figure 1. Theoretical activity volcanoes as a function of relevant descriptors, E_C and E_O, shown for the production of (a) methane, (b) ethanol, and (c) methanol from CO and H_2 on transition metal (211) surfaces. (d–g) Turnover frequencies along the line fitted to the points (E_C, E_O) for Co, CuCo, and Cu resulting in $E_{line} = 1.2*E_C - 0.52$, with fixed $E_O = 0.64*E_C - 1.28$. Reaction conditions are $T = 523$ K and partial pressures of 10 bar of carbon monoxide, 20 bar of hydrogen, 0.01 bar of water, and 0 bar of methane/methanol/ethanol.

preparation conditions, adding promoters, or changing supports.[19−23] However, there is no clear consensus on the structure−activity relationship of bimetallic catalysts and how Co and Cu interact. Many studies claim that the activity and selectivity of catalysts are highly structure sensitive, and step sites, the most common type of defect for metal catalysts, are known to exhibit good activity in many catalytic reactions.[24−26] Yang et al. have shown that the Rh (211) surface is ∼6 orders of magnitude more active than the Rh (111) surface but is highly selective toward methane, while the Rh (111) surface is intrinsically selective toward acetaldehyde.[27] Whether the stepped surface of CuCo has a better activity and selectivity toward ethanol in comparison to the CuCo (111) surface is still elusive.

In this study, the CuCo (211) surface, which displays (111) terraces three atomic rows wide separated by (100) steps, is selected as the model surface for our simulations. At the same time, we chose the CuCo (111) surface to investigate the reactivity of highly coordinated surface sites, since (111) is the surface predominantly exposed under reducing conditions at low pressures.[28] We make a comparative study of the CuCo (211) and the CuCo (111) surfaces using a Cu and Co alloy in a 1:1 ratio. In addition, we focus on the three reaction products methane, ethanol, and methane during CO hydrogenation. Methane and ethanol are taken as representative of hydrocarbons and higher alcohols during the initial stages of CO hydrogenation at low conversion. We have performed density functional theory (DFT) calculations on all possible reaction intermediates in the CO hydrogenation process and used these data together with microkinetic modeling to identify plausible reaction mechanisms and to determine the structure−activity/selectivity relationship.

2. METHODOLOGY

2.1. Density Functional Theory Calculations. All calculations were carried out using Quantum Espresso software,[29] interfaced with the Atomic Simulation Environment (ASE).[30] The BEEF-vdW[31] exchange correlation functional was used because of its accurate estimation of adsorption energies[32] and its explicit inclusion of van der Waals interactions. The fixed bond length (FBL) method was used to identify transition-state structures and their energies. All calculations were performed with a plane-wave cutoff of 500 eV, a density cutoff of 5000 eV, and a Monkhorst−Pack type k-point sampling of 4 × 4 × 1.

A lattice constant of 3.61 Å was calculated for the CuCo alloy by minimizing the energy with respect to unit cell volume. The (211) surface and (111) surface were modeled using periodically repeated unit cells p-(4 × 3) and p-(4 × 2), respectively, with four-layer slabs in the (111) direction in both cases. The two bottom metal layers in the (111) direction were fixed, while the top two layers and the adsorbates were geometrically relaxed so that the maximum force in any direction on any relaxed atom was less than 0.03 eV/Å. The slabs were separated by at least 10 Å of vacuum in the (111) direction. Dipole correction was included in all cases to decouple the electrostatic interaction between periodically repeated slabs. When possible, adsorption and transition-state energies were taken from previously published work.[33]

2.2. Microkinetic Modeling. Microkinetic modeling was carried out using the CatMAP software.[34] Rates were

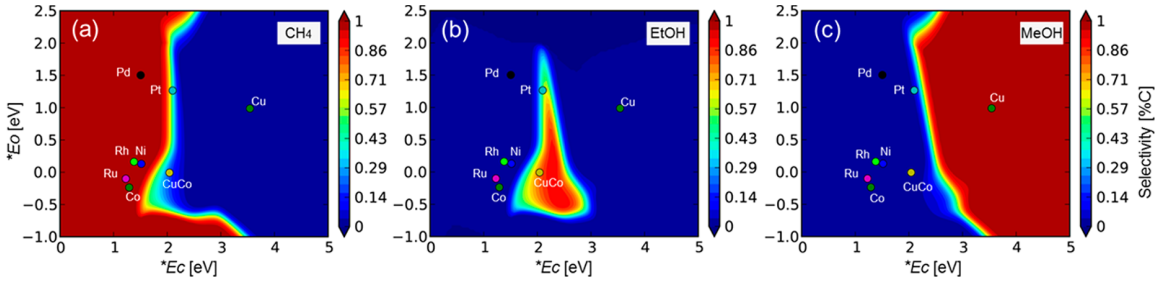

Figure 2. Theoretical selectivity volcanoes for the production of methane, methanol, and ethanol from CO and H_2 on transition metal (211) surfaces. Reaction conditions are identical with those of Figure 1.

determined by numerically solving the coupled differential equations with the steady-state approximation. Selectivity is defined as the rate of formation of the product of interest divided by the rates of formation for methane, methanol, and ethanol without any weighting for the number of carbons. In this work, four different adsorption sites were included on the stepped (211) surface in order to capture the complexity of this reaction (see Scheme S1). The (111) surface was modeled using two surface sites: a "hydrogen reservoir" site and a site for all other intermediates. Further details of the kinetic model are in accordance with previous work.[33]

Binding energies for a given adsorbate were calculated relative to gas-phase H_2, H_2O, and CH_4, defined as

$$*E_{be} = *E_{tot} - *E_{clean} - (x*E_C - y*E_O - z*E_H)$$

where $*E_{tot}$ is the total energy of the adsorbed surface, $*E_{clean}$ is the energy of clean CuCo surfaces, $E_C = E_{CH_4} - 2E_{H_2}$, $E_O = E_{H_2O} - E_{H_2}$, and $E_H = 0.5E_{H_2}$ are relative to the respective gas-phase energies, and x, y, and z are chosen to represent the number of carbon, oxygen, and hydrogen atoms in the adsorbed intermediate.

By using standard vibrational corrections within the harmonic oscillator approach and a frozen slab approximation, vibrational frequencies were computed using a finite difference approximation to the Hessian and subsequent diagonalization to find the normal modes, as implemented in ASE. From the vibrational frequencies, zero-point energy (ZPE) corrections were included and the entropy and enthalpy under reaction conditions were determined. The change in free energy is given by

$$\Delta G = \Delta E + \Delta E_{ZPE} + \Delta C_{v\_harm}^{0\rightarrow T} - T\Delta S$$

where ΔE is the reaction energy of each intermediate step, ΔE_{ZPE} is the zero-point energy correction, ΔC is the enthalpy correction, ΔS is the entropy change, and T is the absolute temperature.

3. RESULTS AND DISCUSSION

3.1. Syngas Conversion on CuCo (211). Scaling relations[35] between energies of adsorbates and transition states and reaction energies are used to reduce the parameter space for our screening studies, and this approach allows us to model the CO hydrogenation using only two parameters, the carbon and oxygen binding energies. The established scaling relations are shown in Figure S1 in the Supporting Information. Herein we build a microkinetic model for the CO hydrogenation on (211) transition-metal surfaces similarly to our earlier work.[33] The developed descriptor-based microkinetic model for CO hydrogenation is used to visualize trends for the different product formation rates and to gain a better understanding of the properties of CuCo alloy catalysts.

Figure 1 gives a description of the activity volcanoes for the production of methane, methanol, and ethanol from CO and H_2 on transition-metal (211) surfaces. It can be observed from Figure 1a–c that the calculated values of E_C and E_O on CuCo (211) are located very close to the maximum of the ethanol volcano. In addition, the turnover frequency of ethanol on CuCo (211) is higher than that of methane and methanol. These results indicate that CuCo (211) is more selective toward ethanol formation, as confirmed by the selectivity volcanoes (see Figure 2). CuCo has the highest ethanol selectivity of 65%, with the remainder being 30% toward methane and 5% toward methanol. At the same time, it is also found from Figure 2 that pure Co is selective toward methane, while pure Cu is selective toward methanol. The above analysis indicates that CuCo alloy is a promising catalyst candidate for ethanol formation.

To further justify why a CuCo alloy surface is believed to be more selective toward ethanol formation in comparison to pure Co and pure Cu, a straight line (the black solid line) between copper and cobalt on the activity volcano is drawn. This line on the 2D volcano plot is translated into a one-dimensional axis, which is described by a linear combination of carbon and oxygen binding energies. From a simple energy interpolation scheme an alloy formed between Cu and Co should fall on this line. The turnover frequency of the three products along the line is shown in Figure 1d–g. A high methane formation rate appears at strong carbon binding (Figure 1d). In this region, CO dissociation via a hydrogen-assisted single reaction step can easily be achieved.[36] An appreciable rate of methanol formation appears in less reactive regions (see Figure 1f), where CO cannot be split as easily and hence is hydrogenated first.

The maximum ethanol formation rate is naturally located at moderate carbon binding energies between the maxima of methane and methanol production rates. For a direct comparison, the three product rate figures (Figure 1d–f) have been merged into one, as shown in Figure 1g along the fitted line. It can be observed that the ethanol formation rate is higher than that of methane and methanol at the binding energy between points A and B, which means that in this region ethanol is the main product. Similarly to the above analysis, higher selectivity toward methane or methanol occurs where the binding energy is stronger than at energy point A or weaker than at energy point B, respectively. Hence, the selectivity for ethanol to happen is the highest between points A and B, as shown in Figure 3. From coverage maps of C* and

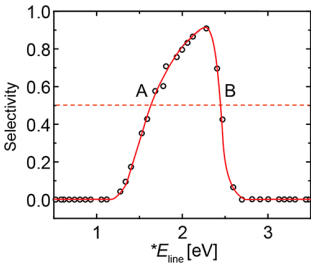

Figure 3. Calculated selectivity of ethanol along the line fitted to the points (E_C, E_O) for Co, CuCo, and Cu.

CO* (Figure S2a,b), we observe that both C* and CO* have high coverage in this region, meaning that ethanol formation requires both dissociated CO and adsorbed CO.

For pure Co (211), dissociation of CO is favored, leading to a high coverage of carbon on the surface (see Figure S2a). This greatly promotes methane formation. On pure Cu, the coverage of CO is dominant and no atomic carbon can be formed because of the high barrier for CO dissociation. Hence, only methanol by direct CO hydrogenation is being produced. Since the carbon and oxygen binding energies on the CuCo surface are moderate, both C* and CO* coexist on the surface, leading to a higher production rate of ethanol. In other words, metallic Co has a strong capability in breaking the C−O bond to produce a large number of CH_x species. The presence of Cu weakens the dissociation of CO due to the modification of electronic structure of Co sites by Cu atoms and then limits the formation of CH_x species, enhancing the ratio of nondissociated CO/dissociated CO on the catalyst surface.

A detailed investigation for the stable adsorption configurations of all possible adsorbed species involved in the formations of methane, methanol, and ethanol has been carried out on the CuCo(211) surface, and the corresponding adsorption energies and energy barriers are given in Table S1. The most favorable pathways for CO hydrogenation to methane, methanol, and ethanol on the CuCo (211) surface are shown in Figure 4. Hydrogenation of CO to methanol occurs most efficiently through HCO*, CH_2O*, CH_3O*, and finally CH_3OH*. In this sequence of reactions, the highest free energy barrier is the last hydrogenation step, $CH_3O^* + H^* \rightarrow CH_3OH^*$. This result is in good agreement with theoretical observations on Co-decorated Cu alloy catalysts.[37]

For the chain growth toward higher alcohols, an important reaction step is the dissociation of CO. In the literature,[36] four common pathways for CO dissociation have been reported: direct dissociation (CO* ↔ C* + O*), COH* (CO* + H* ↔ COH* ↔ C* + OH*), CHO* (CO* + H* ↔ CHO* ↔ CH* + O*), and a hydrogen-assisted one-step dissociation of CO (CO* + H* ↔ C* + OH*). We have calculated the energy needed to split CO through each of these four pathways on the CuCo surface and found barriers of 2.8, 2.4, 2.0, and 1.3 eV, respectively. Clearly, the hydrogen-assisted pathway is the dominant route in agreement with earlier studies.[24,38] The resulting surface carbon species can be stepwise hydrogenated to yield CH*, CH_2*, CH_3*, and ultimately methane. We have identified that the CH_2* intermediate species can couple with CO* /CHO* with a comparable barrier to further hydrogenation. It is this creation of a CH_2CO* /CH_2CHO* backbone that can lead to the formation of ethanol.

Recently, more studies[37,39,40] have proven that HCO insertion occurs more easily because of a lower activation

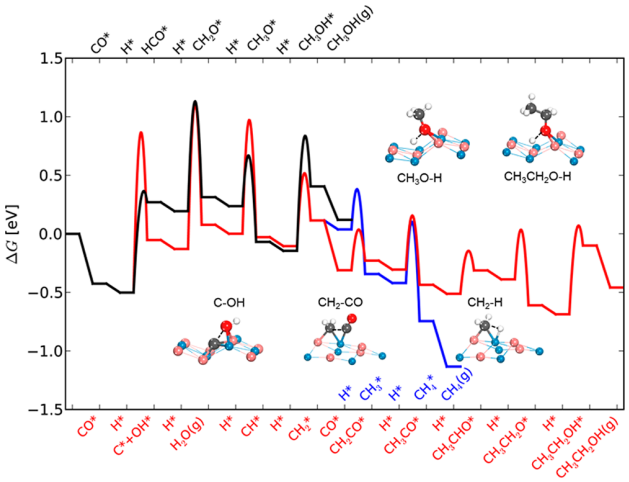

Figure 4. Free energy diagrams of methane (blue), methanol (black), and ethanol (red) formation at 523 K on the CuCo(211) surface. Free energies of reactants (CO, H_2) are computed at a pressure of 20 bar and H_2:CO = 2; all other free energies are computed at the standard state. Insets are DFT optimized geometries of key transition states.

energy barrier. Therefore, it is considered a key reaction step in the ethanol formation on bimetallic Cu-Co catalyst. Our calculations also demonstrate that the energy barrier of forming CH_2CHO* from CH_2 and CHO (0.28 eV) is lower than that of forming CH_2CO* (0.37 eV). However, as seen in Figure S3b,c, the coverage of CHO* is ∼6 orders of magnitude lower than the coverage of CO* on the CuCo surface. Hence, the chain growth via CHO insertion occurs at a much lower rate due to coverage restrictions of CHO* under steady-state conditions. We therefore conclude that CO insertion is the dominant pathway for chain growth toward higher alcohols on CuCo (211).

Inspection of the overall energetics of the free energy diagram in Figure 4 indicates a close competition between the CH_2* hydrogenation to methane and coupling with CO to produce ethanol as the two steps in the reaction that determine the overall product selectivity. However, the free energy barrier of CH_2* hydrogenation to CH_3* is 0.39 eV, while that of CH_2/CO coupling is 0.37 eV. It is rather difficult to make predictions about selectivity in such a complex multistep process from the free energy diagrams alone. Therefore, an investigation on the activity and selectivity is performed using a microkinetic model. At the same time, the barrier of coupling of CH_2* with itself to form ethylene is calculated to be 1 eV; this is thus unfavorable and was not considered for the microkinetic model.

Figure 5 summarizes the calculated turnover frequencies (TOFs) and corresponding selectivities for methane, ethanol, and methanol production. As expected, TOFs of these three products (Figure 5a−c) increase with increasing temperature. Figure 5d,e shows a decrease in methane selectivity and an increase in ethanol selectivity with increasing pressure between 500 and 600 K, which can be explained by a more favorable CH_2/CO coupling step in comparison to the CH_2 hydrogenation step at high CO coverage. This also indicates that, with increasing temperature, the selectivity of ethanol decreases while that of methane increases, in agreement with available experimental results.[20,42]

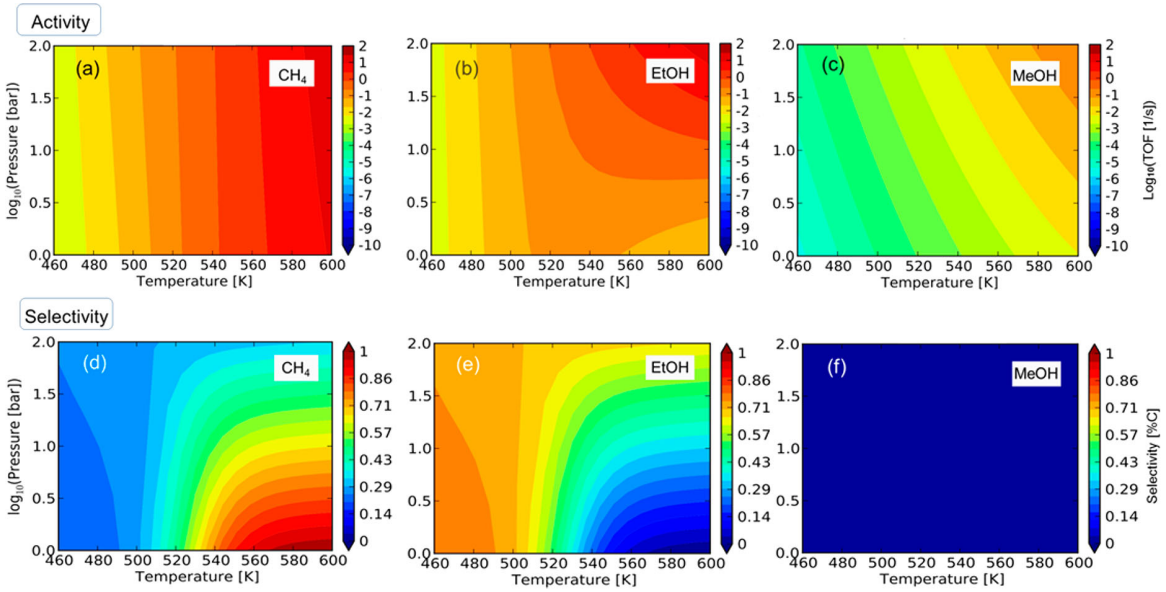

Figure 5. Turnover frequencies (a–c) and carbon selectivities (d–f) for methane, ethanol, and methanol calculated using the microkinetic model for CuCo (211). The reaction conditions are P_{H_2}:P_{CO} = 2 and P_{H_2O} = P_{CH_4} = P_{MeOH} = P_{EtOH} ≈ 0 bar.

To better depict the trend, a plot of rate/selectivity versus temperature at 20 bar is given in Figure S3. Interestingly, the change in selectivity with temperature can clearly be explained on the basis of thermodynamic arguments. From the Gibbs free energy of formation (ΔG_f) of the three products in Figure S4, we find that the ΔG_f value of ethanol is lower than that of methane at T < 500 K. Hence, at low temperatures, ethanol production is thermodynamically favored, and thus the reaction rate of ethanol is the fastest. Upon an increase in temperature, methane formation gradually becomes thermodynamically more favorable, resulting in an increased methane selectivity in comparison to ethanol. Above 700 K, thermodynamics dominates and methane is the main product. We note that ethanol is the main product under typical experimental conditions (503–573 K, 20–40 bar). The formation of methanol is both thermodynamically and kinetically less favorable than the formation of methane or ethanol, as seen from the activity and selectivity plots in Figure 5c,f.

On the basis of the above analysis from the microkinetic modeling, it can be concluded that the CuCo (211) surface is selective toward ethanol under experimental conditions, and methane becomes more favorable at higher temperatures, which is consistent with the results we predicted with the initial screening study through Catmap. Adsorbate and transition-state energies calculated on our CuCo model surfaces fit scaling relations well. Hence, the scaling relations apply not only to pure metals but also to bimetallic catalysts. We can therefore use it to speculate on the reactivity of bimetallic surfaces and predict other promising HAS catalysts, by simply calculating the binding energy of carbon and oxygen on bimetallic catalysts and check whether it is located in the selective region of ethanol formation.

3.2. Syngas Conversion on CuCo (111). On the basis of a detailed analysis of the CuCo 211) surface, a high selectivity toward ethanol is predicted for that surface orientation. Considering that the stepped (211) surface is less stable and therefore less abundant than lower Miller index surfaces, we therefore chose to explore the reaction mechanism for CO hydrogenation on the close-packed CuCo (111) surface, a facet that is commonly detected by experiments.[42]

Similarly to the (211) surface, scaling relations are applied that allow us to build a descriptor-based microkinetic model that only depends on two descriptors. For the (111) surfaces CO and OH binding energies were chosen, as they are adsorbates occurring in the reaction mechanism and scale especially well with the early reaction intermediates. The established scaling relations are shown in Figure S5. Parameter settings and the reaction network for the (111) surface were taken from the literature.[27,43] Methanol is predicted to be the main product on the CuCo(111) surface (see Figure S6a–c). It can be seen clearly from the selectivity volcanoes (see Figure S6d–f) that the methanol selectivity on CuCo is more than 90%. In order to confirm our prediction, a detailed study of the reaction mechanism of CO hydrogenation on the CuCo (111) surface is conducted.

As shown in the free energy diagram in Figure 6, the (111) surface favors the direct hydrogenation of CO to methanol, which is identical with that found on the (211) surface. For the methanation pathway, we find a difference in the intermediate leading to the C–O bond cleavage on the two surfaces. The CH_x* species on the (111) surface is obtained via splitting of the C–O bond in the adsorbed methoxy intermediate (CH_3O*), while on the (211) surface it is obtained through H-assisted dissociation of CO. The (111) surface is less reactive than the (211) surface, thus making it difficult to break the C–O bond directly. The resulting CH_3* species can either be hydrogenated to yield methane or alternatively couple with CO* to produce CH_3CO* as an intermediate in the ethanol formation. Our calculations identify the dissociation of CH_3O* into CH_3* and O* as the reaction step with the highest free energy barrier.

As shown in Figure 7a, the rate of CO hydrogenation to methanol is about 10^{-5} turnover/s at 523 K and 20 bar, while the rates for ethanol and methane are ~10^{-13} and ~10^{-8} turnover/s under these conditions, respectively. The funda-

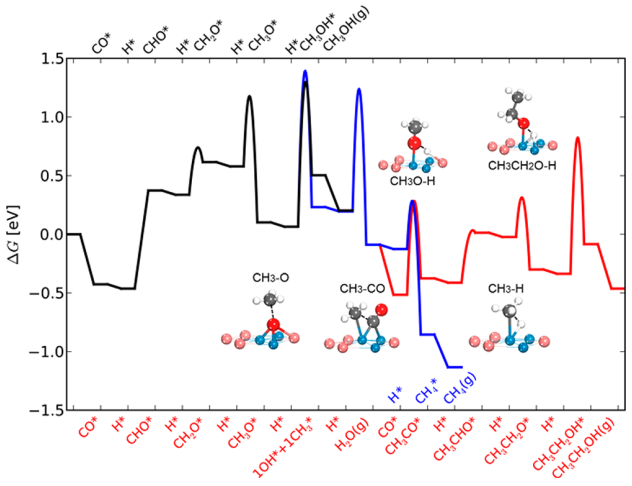

Figure 6. Free energy diagrams of methane (blue), methanol (black), and ethanol (red) formation at 523 K on the CuCo (111) surface. Free energies of reactants (CO, H_2) are computed at a pressure of 20 bar and H_2:CO = 2:1; all other free energies are computed at the standard state.

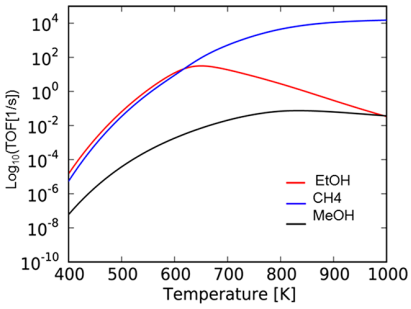

Figure 8. Turnover frequencies for ethanol (red) and methane (blue) using the microkinetic model for CuCo (211) and turnover frequencies for methanol (black) using the microkinetic model for CuCo (111). The reaction conditions are P_{H_2} = 6.66 bar, P_{CO} = 13.33 bar, and $P_{H_2O} = P_{CH_4} = P_{MeOH} = P_{EtOH} \approx 0$ bar.

mental reason for this results is that the splitting of the C−O bond from surface CH_3O* is too difficult due to a high barrier. This results in a low coverage of C_1 species on the surface and therefore low rates for methane formation and C−C coupling reactions. Methanol is therefore the primary product on the CuCo (111) surface, as shown in the selectivity map (see Figure 7b).

3.3. Comparisons with Experimental Results. To better analyze the three products on the CuCo alloy, turnover frequencies for the ethanol and methane on the (211) surface and for the methanol on the (111) surface are described in Figure 8. The ethanol production on the (211) surface is calculated to be about 10^{-1} s^{-1} at 523 K, whereas the methanol is produced at a much lower rate on the (111) surface (10^{-4} s^{-1} at 523 K). Although the number of step sites is much smaller than that of terrace sites (1−2 orders of magnitude) on the CuCo alloy surface, the turnover frequency of the ethanol on the CuCo step is approximately 3 orders of magnitude higher than the methanol rate on the terrace. Thus, the formation rate of ethanol on a typical (2−10 nm) CuCo catalyst particle should be higher than for methanol.

The predictions above are supported by our experimental results,[15] in which CuCo alloy catalysts are prepared by calcining and reducing LDH precursors and used for HAS. The catalytic performance of the CuCo alloy catalysts with a Cu:Co ratio of 1:1 shows that the carbon selectivity of ethanol is more than 8 times higher than that of methanol at 523 K, 3 MPa, and a GHSV value of 3900 mL $(g_{cat}\ h)^{-1}$, in good agreement with the trend of predicted product selectivity.

Meanwhile, with increasing temperature, the TOF of ethanol production is gradually decreasing below that of methane formation, resulting in the decrease in ethanol selectivity, while that of methane increases, which is consistent with available experimental results.[20,41] In addition, the experimental results[15] also show that, with increasing cobalt content in the CuCo-based catalysts, the selectivity toward methane increases. At a Co:Cu ratio of about 2:1, the catalyst shows the highest alcohol selectivity, with a CO conversion of 51.8%, a selectivity to alcohols of 45.8%, and 94.3 wt % of total C_{2+}OH alcohol production. As for the relation between the CuCo surface and Cu:Co ratio, our group will follow up on this in depth in subsequent research.

4. CONCLUSION

In this work, DFT and microkinetic modeling are employed in a mechanistic study of the CO hydrogenation process on a stepped (211) and close-packed (111) CuCo alloy surface. We have studied the reaction of CO and H_2 into methane, methanol, and ethanol in detail, and we have found the following.

(a) Methanol is produced by direct hydrogenation of nondissociated CO, methane by hydrogenation of surface CH_x* species, and ethanol requires insertion of CO into CH_x* followed by hydrogenation. The ability to break the CO bond

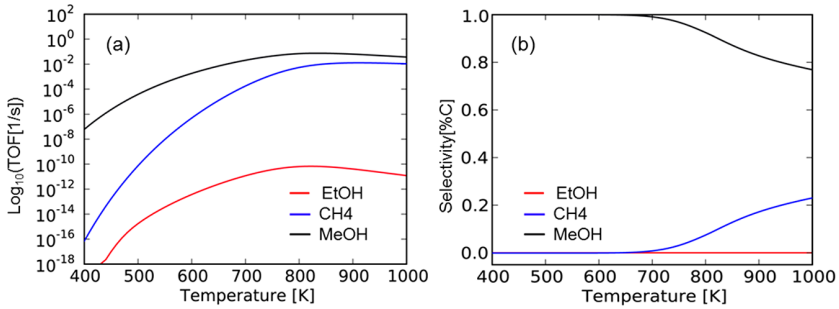

Figure 7. Turnover frequencies (a) and carbon selectivities (b) for methane (blue), ethanol (red), and methanol (black) using the microkinetic model for CuCo (111). The reaction conditions are 523 K, P_{H_2} = 6.66, P_{CO} = 13.33, and $P_{H_2O} = P_{CH_4} = P_{MeOH} = P_{EtOH} \approx 0$ bar.

identifies the difference in products on stepped and close-packed surfaces, and the barriers to subsequent hydrogenation or CO coupling of CH_x* on the surfaces define the selectivity toward methane or ethanol. The CH_x* species are produced by a hydrogen-assisted dissociation of CO on the CuCo (211) surface and by dissociation of CH_3O* on the (111) surface.

(b) The activity and selectivity volcanoes obtained from our microkinetic analysis show that a CuCo alloy is a promising candidate catalyst for formation of ethanol. We have found that calculated adsorption and transition-state energies on the CuCo surfaces follow proposed scaling relations for (111) and (211) surfaces. This suggests that scaling relations will apply equally well to other bimetallic systems, thus allowing us to explore other promising bimetallic catalysts.

(c) We find the selectivity to be very structure sensitive. The CuCo (211) surface is active and selective toward ethanol under typical reaction conditions, and at elevated temperatures methane production becomes favorable. The CuCo (111) surface is selective toward methanol, but with a low rate. The high activity and selectivity toward ethanol on the (211) surface are mainly due to the lower C−O dissociation barrier and the high rate of CH_x−CO coupling.

This improved atomic-scale understanding of CuCo catalysts provides a framework for understanding the activity and selectivity patterns of more complex catalysts. In turn, this will prove very useful for computational design and optimizations of other bimetallic catalysts.

AUTHOR INFORMATION

Corresponding Authors

*E-mail for F.A.-P.: abild@slac.stanford.edu.
*E-mail for J.K.N.: norskov@stanford.edu.

ORCID

Ang Cao: 0000-0003-3787-6949
Julia Schumann: 0000-0002-4041-0165
Yuan Liu: 0000-0001-9785-8799
Frank Abild-Pedersen: 0000-0002-1911-074X

Notes

The authors declare no competing financial interest.

■ ACKNOWLEDGMENTS

A.C. and Y.L. gratefully acknowledge financial support from the China Scholarship Council. J.S. thanks the German Academic Exchange Service (DAAD) for support through a postdoc fellowship. A.C., J.S., T.W, L.Z., J.X., P.B., F.A-P., and J.K.N. acknowledge support from the U.S. Department of Energy, Office of Basic Energy Sciences, to the SUNCAT Center for Interface Science and Catalysis at SLAC National Accelerator Laboratory and Stanford University.

REFERENCES

(1) Gong, J.; Yue, H.; Zhao, Y.; Zhao, S.; Zhao, L.; Lv, J.; Wang, S.; Ma, X. Synthesis of ethanol via syngas on Cu/SiO_2 catalysts with balanced Cu^0-Cu^+ sites. *J. Am. Chem. Soc.* **2012**, *134*, 13922−13925.

(2) Luk, H. T.; Mondelli, C.; Ferre, D. C.; Stewart, J. A.; PerezRamirez, J. Status and prospects in higher alcohols synthesis from syngas. *Chem. Soc. Rev.* **2017**, *46*, 1358−1426.

(3) Wang, L. X.; Wang, L.; Zhang, J.; Liu, X. L.; Wang, H.; Zhang, W.; Yang, Q.; Ma, J. Y.; Dong, X.; Yoo, S. J.; Kim, J. G.; Meng, X. J.; Xiao, F. S. Selective Hydrogenation of CO_2 to Ethanol over Cobalt Catalysts. *Angew. Chem., Int. Ed.* **2018**, *57*, 6104−6108.

(4) Su, J.; Zhang, Z.; Fu, D.; Liu, D.; Xu, X. C.; Shi, B.; Wang, X.; Si, R.; Jiang, Z.; Xu, J.; Han, Y. F. Higher alcohols synthesis from syngas over CoCu/SiO2 catalysts: Dynamic structure and the role of Cu. *J. Catal.* **2016**, *336*, 94−106.

(5) Zhao, Y.; Yang, M.; Sun, D.; Su, H.; Sun, K.; Ma, X.; Bao, X.; Li, W. Rh-Decorated Cu Alloy Catalyst for Improved C_2 Oxygenate Formation from Syngas. *J. Phys. Chem. C* **2011**, *115*, 18247−18256.

(6) Zhao, Y. H.; Sun, K.; Ma, X.; Liu, J.; Sun, D.; Su, H. Y.; Li, W. X. Carbon chain growth by formyl insertion on rhodium and cobalt catalysts in syngas conversion. *Angew. Chem., Int. Ed.* **2011**, *50*, 5335−5538.

(7) Wen, G.; Wang, Q.; Zhang, R.; Li, D.; Wang, B. Insight into the mechanism about the initiation, growth and termination of the C-C chain in syngas conversion on the Co(0001) surface: a theoretical study. *Phys. Chem. Chem. Phys.* **2016**, *18*, 27272−27283.

(8) Wang, Z.; Kumar, N.; Spivey, J. J. Preparation and characterization of lanthanum-promoted cobalt−copper catalysts for the conversion of syngas to higher oxygenates: Formation of cobalt carbide. *J. Catal.* **2016**, *339*, 1−8.

(9) Wang, J.; Zhang, X.; Sun, Q.; Chan, S.; Su, H. Chain growth mechanism on bimetallic surfaces for higher alcohol synthesis from syngas. *Catal. Commun.* **2015**, *61*, 57−61.

(10) Behrens, M.; Studt, F.; Kasatkin, I.; Kühl, S.; Hävecker, M.; Abild-Pedersen, F.; Zander, S.; Girgsdies, F.; Kurr, P.; Kniep, B.-L.; Tovar, M.; Fischer, R. W.; Nørskov, J. K.; Schlögl, R. The Active Site of Methanol Synthesis over $Cu/ZnO/Al_2O_3$ Industrial Catalysts. *Science* **2012**, *336*, 893−897.

(11) Studt, F.; Behrens, M.; Kunkes, E. L.; Thomas, N.; Zander, S.; Tarasov, A.; Schumann, J.; Frei, E.; Varley, J. B.; Abild-Pedersen, F.; Nørskov, J. K.; Schlögl, R. The Mechanism of CO and CO_2 Hydrogenation to Methanol over Cu-Based Catalysts. *ChemCatChem* **2015**, *7*, 1105−1111.

(12) Liu, J. X.; Su, H. Y.; Sun, D. P.; Zhang, B. Y.; Li, W. X. Crystallographic dependence of CO activation on cobalt catalysts: HCP versus FCC. *J. Am. Chem. Soc.* **2013**, *135*, 16284−16287.

(13) Fang, Y. Z.; Liu, Y.; Zhang, L. H. $LaFeO_3$-supported nano Co-Cu catalysts for higher alcohol synthesis from syngas. *Appl. Catal., A* **2011**, *397*, 183−191.

(14) Bailliard-Letournel, R. M.; Gomez Cobo, A. J.; Mirodatos, C.; Primet, M. Dalmon, J. A., About the nature of the Co-Cu interaction in Co-based catalysts for higher alcohols synthesis. *Catal. Lett.* **1989**, *2*, 149−156.

(15) Cao, A.; Liu, G.; Yue, Y.; Zhang, L.; Liu, Y. Nanoparticles of Cu−Co alloy derived from layered double hydroxides and their catalytic performance for higher alcohol synthesis from syngas. *RSC Adv.* **2015**, *5*, 58804−58812.

(16) Cao, A.; Liu, G.; Wang, L.; Liu, J.; Yue, Y.; Zhang, L.; Liu, Y. Growing layered double hydroxides on CNTs and their catalytic performance for higher alcohol synthesis from syngas. *J. Mater. Sci.* **2016**, *51*, 5216−5231.

(17) Tien-Thao, N.; Alamdari, H.; Zahedi-Niaki, M. H.; Kaliaguine, S. $LaCo_{1-x}Cu_xO_{3-\delta}$ perovskite catalysts for higher alcohol synthesis. *Appl. Catal., A* **2006**, *311*, 204−212.

(18) Nguyen, T. T.; Zahedi-Niaki, M. H.; Alamdari, H.; Kaliaguine, S., Co-Cu Metal Alloys from $LaCo_{1-x}Cu_xO_3$ Perovskites as Catalysts for Higher Alcohol Synthesis from Syngas. *Int. J. Chem. React. Eng.* **2007**, *5*. DOI: 10.2202/1542-6580.1583

(19) Prieto, G.; Beijer, S.; Smith, M. L.; He, M.; Au, Y.; Wang, Z.; Bruce, D. A.; de Jong, K. P.; Spivey, J. J.; de Jongh, P. E. Design and synthesis of copper-cobalt catalysts for the selective conversion of synthesis gas to ethanol and higher alcohols. *Angew. Chem., Int. Ed.* **2014**, *53*, 6397−6401.
(20) Wang, Z.; Kumar, N.; Spivey, J. J, Preparation and characterization of lanthanum-promoted cobalt−copper catalysts for the conversion of syngas to higher oxygenates: Formation of cobalt carbide. *J. Catal.* **2016**, *339*, 1−8.
(21) Liu, G.; Niu, T.; Pan, D.; Liu, F.; Liu, Y. Preparation of bimetal Cu−Co nanoparticles supported on meso−macroporous SiO_2 and their application to higher alcohols synthesis from syngas. *Appl. Catal., A* **2014**, *483*, 10−18.
(22) Ao, M.; Pham, G. H.; Sunarso, J.; Tade, M. O.; Liu, S. Active Centers of Catalysts for Higher Alcohol Synthesis from Syngas: A Review. *ACS Catal.* **2018**, *8*, 7025−7050.
(23) Gupta, M.; Smith, M. L.; Spivey, J. J. Heterogeneous Catalytic Conversion of Dry Syngas to Ethanol and Higher Alcohols on Cu-Based Catalysts. *ACS Catal.* **2011**, *1*, 641−656.
(24) Andersson, M. P.; Abild-Pedersen, F.; Remediakis, I. N.; Bligaard, T.; Jones, G.; Engbæk, J.; Lytken, O.; Horch, S.; Nielsen, J. H.; Sehested, J.; Rostrup-Nielsen, J. R.; Nørskov, J. K.; Chorkendorff, I. Structure sensitivity of the methanation reaction: H_2-induced CO dissociation on nickel surfaces. *J. Catal.* **2008**, *255*, 6−19.
(25) Perez-Gallent, E.; Marcandalli, G.; Figueiredo, M. C.; Calle-Vallejo, F.; Koper, M. T. M. Structure- and Potential-Dependent Cation Effects on CO Reduction at Copper Single-Crystal Electrodes. *J. Am. Chem. Soc.* **2017**, *139*, 16412−16419.
(26) Zhong, L.; Yu, F.; An, Y.; Zhao, Y.; Sun, Y.; Li, Z.; Lin, T.; Lin, Y.; Qi, X.; Dai, Y.; Gu, L.; Hu, J.; Jin, S.; Shen, Q.; Wang, H. Cobalt carbide nanoprisms for direct production of lower olefins from syngas. *Nature* **2016**, *538*, 84−87.
(27) Yang, N.; Medford, A. J.; Liu, X.; Studt, F.; Bligaard, T.; Bent, S. F.; Norskov, J. K. Intrinsic Selectivity and Structure Sensitivity of Rhodium Catalysts for C_{2+} Oxygenate Production. *J. Am. Chem. Soc.* **2016**, *138*, 3705−3714.
(28) Su, J.; Mao, W.; Xu, X.-C.; Yang, Z.; Li, H.; Xu, J.; Han, Y.-F. Kinetic study of higher alcohol synthesis directly from syngas over $CoCu/SiO_2$ catalysts. *AIChE J.* **2014**, *60*, 1797−1809.
(29) Giannozzi, P.; Baroni, S.; Bonini, N.; Calandra, M.; Car, R.; Cavazzoni, C.; Ceresoli, D.; Chiarotti, G. L.; Cococcioni, M.; Dabo, I.; Dal Corso, A.; de Gironcoli, S.; Fabris, S.; Fratesi, G.; Gebauer, R.; Gerstmann, U.; Gougoussis, C.; Kokalj, A.; Lazzeri, M.; Martin-Samos, L.; Marzari, N.; Mauri, F.; Mazzarello, R.; Paolini, S.; Pasquarello, A.; Paulatto, L.; Sbraccia, C.; Scandolo, S.; Sclauzero, G.; Seitsonen, A. P.; Smogunov, A.; Umari, P.; Wentzcovitch, R. M. QUANTUM ESPRESSO: a modular and open-source software project for quantum simulations of materials. *J. Phys.: Condens. Matter* **2009**, *21*, 395502.
(30) Bahn, S. R.; Jacobsen, K. W. An object-oriented scripting interface to a legacy electronic structure code. *Comput. Sci. Eng.* **2002**, *4*, 56−66.
(31) Wellendorff, J.; Lundgaard, K. T.; Møgelhøj, A.; Petzold, V.; Landis, D. D.; Nørskov, J. K.; Bligaard, T.; Jacobsen, K. W. Density functionals for surface science: Exchange-correlation model development with Bayesian error estimation. *Phys. Rev. B: Condens. Matter Mater. Phys.* **2012**, *85*, 235149.
(32) Wellendorff, J.; Silbaugh, T. L.; Garcia-Pintos, D.; Nørskov, J. K.; Bligaard, T.; Studt, F.; Campbell, C. T. A benchmark database for adsorption bond energies to transition metal surfaces and comparison to selected DFT functionals. *Surf. Sci.* **2015**, *640*, 36−44.
(33) Medford, A. J.; Lausche, A. C.; Abild-Pedersen, F.; Temel, B.; Schjødt, N. C.; Nørskov, J. K.; Studt, F. Activity and Selectivity Trends in Synthesis Gas Conversion to Higher Alcohols. *Top. Catal.* **2014**, *57*, 135−142.
(34) Medford, A. J.; Shi, C.; Hoffmann, M. J.; Lausche, A. C.; Fitzgibbon, S. R.; Bligaard, T.; Nørskov, J. K. CatMAP: A Software Package for Descriptor-Based Microkinetic Mapping of Catalytic Trends. *Catal. Lett.* **2015**, *145*, 794−807.
(35) Abild-Pedersen, F.; Greeley, J.; Studt, F.; Rossmeisl, J.; Munter, T. R.; Moses, P. G.; Skúlason, E.; Bligaard, T.; Nørskov, J. K. Scaling Properties of Adsorption Energies for Hydrogen-Containing Molecules on Transition-Metal Surfaces. *Phys. Rev. Lett.* **2007**, *99*, 016105.
(36) Lausche, A. C.; Medford, A. J.; Khan, T. S.; Xu, Y.; Bligaard, T.; Abild-Pedersen, F.; Nørskov, J. K.; Studt, F. On the effect of coverage-dependent adsorbate−adsorbate interactions for CO methanation on transition metal surfaces. *J. Catal.* **2013**, *307*, 275−282.
(37) Zhang, R.; Liu, F.; Wang, B. Co-decorated Cu alloy catalyst for C_2 oxygenate and ethanol formation from syngas on Cu-based catalyst: insight into the role of Co and Cu as well as the improved selectivity. *Catal. Sci. Technol.* **2016**, *6*, 8036−8054.
(38) Andersson, M. P.; Bligaard, T.; Kustov, A.; Larsen, K. E.; Greeley, J.; Johannessen, T.; Christensen, C. H.; Nørskov, J. K. Toward computational screening in heterogeneous catalysis: Pareto-optimal methanation catalysts. *J. Catal.* **2006**, *239*, 501−506.
(39) Zhang, M.; Yao, R.; Jiang, H.; Li, G.; Chen, Y. Catalytic activity of transition metal doped Cu(111) surfaces for ethanol synthesis from acetic acid hydrogenation: a DFT study. *RSC Adv.* **2017**, *7*, 1443−1452.
(40) Ren, B.; Dong, X.; Yu, Y.; Wen, G.; Zhang, M. A density functional theory study on the carbon chain growth of ethanol formation on Cu-Co (111) and (211) surfaces. *Appl. Surf. Sci.* **2017**, *412*, 374−384.
(41) Xiang, Y.; Kruse, N. Cobalt−copper based catalysts for higher terminal alcohols synthesis via Fischer−Tropsch reaction. *J. Energy Chem.* **2016**, *25*, 895−906.
(42) Liu, G. L.; Niu, T.; Cao, A.; Geng, Y. X.; Zhang, Y.; Liu, Y. The deactivation of Cu−Co alloy nanoparticles supported on ZrO_2 for higher alcohols synthesis from syngas. *Fuel* **2016**, *176*, 1−10.
(43) Schumann, J.; Medford, A. J.; Yoo, J. S.; Zhao, Z. J.; Bothra, P.; Cao, A.; Studt, F.; Abild-Pedersen, F.; Nørskov, J. K. Selectivity of Synthesis Gas Conversion to C_{2+} Oxygenates on fcc(111) Transition-Metal Surfaces. *ACS Catal.* **2018**, *8*, 3447−3453.